COBEM 99
XV Congresso Brasileiro de Engenharia Mecânica
15th Brazilian Congress of Mechanical Engineering
22 - 26 de Novembro de 1999 / November 22 - 26, 1999 Águas de Lindóia, São Paulo,

A CONTROL VOLUME-FINITE ELEMENT METHOD (CVFEM) FOR UNSTEADY FLUID FLOWS

João B. Campos Silva
João B. Aparecido
Universidade Estadual Paulista, Faculdade de Engenharia de Ilha Solteira, Departamento de Engenharia Mecânica
Cx.P. 31 - 15385-000 - Ilha Solteira, SP, Brasil
Luiz F. M. Moura
Universidade Estadual de Campinas, Faculdade de Engenharia Mecânica, Departamento de Engenharia Térmica e de Fluidos
Cx. P. 6122 - 13083-970 - Campinas, SP, Brasil

Abstract. *A control volume-finite element method (CVFEM) to simulate unsteady, incompressible and viscous fluid flows using nine-noded quadrilateral elements has been developed. The mathematical model of the flows is constituted by the Navier-Stokes equations in primitive variables u-v-p. A technique of upwind known as MAW - Mass Weighted Interpolation was extended for the finite element implemented in this work. The set of nonlinear partial differential equations was integrated and after using interpolation functions and time discretization, the algebraic system of equations was solved by using the frontal method. The results obtained for some benchmark problems compared favorably with available results from the literature.*

Keywords: Finite element method, Control volume, Navier-Stokes equations, Primitive variables, Computational fluid dynamics.

1. INTRODUCTION

Flows of fluids are of interest in many applications of engineering and nature. Those flows that are governed by a set of non-linear partial differential equations of convection-diffusion type, generally, occur in domains with geometrical complexity. In this way, practical solutions must be obtained through numerical techniques such as: The Finite Difference Method (FDM), the Finite Volume Method (FVM) and/or the Finite Element Method (FEM). During last decades, the finite element method has been improved for using in the area of Computational Fluid Dynamics (CFD) constituting a powerful tool to simulate complicated situations of fluid flows due to its versatility to discretize complex geometry. Nonetheless, the finite volume method is the most used method to calculate fluid flows. The control volume-finite element method (CVFEM) combines attractive characteristics from both the finite element and the finite volume methods. In this work, some results obtained by using a quadratic, quadrilateral nine-noded element for unsteady, incompressible and viscous thermal fluid flows are presented. The CVFEM was presented by Baliga and Patankar (1980, 1983) using linear triangular finite elements and by Raw and Schneider (1986) using linear quadrilateral elements. Several authors have enhanced the CVFEM since that time till nowadays. Raw et al. (1985) applied the nine-noded element to solve pure heat conduction problems. Banaszek (1989) did a comparison of the Galerkin and CVFEM methods in diffusion problems using six-noded and nine-noded elements. Campos Silva (1998) developed a solver based on the nine-noded finite element and a control volume formulation to simulate 2D transient, incompressible, viscous fluid flows. During the development of the work of Campos Silva (1998), some results were presented by Campos Silva and Moura (1997) and Campos Silva et al. (1998).

The CVFEM combines the flexibility of the finite element methods to discretize complex geometry with the conservative formulation of the finite volume methods in which the variables have an easy physical interpretation in terms of fluxes, forces and sources. Saabas and Baliga (1994) presented a list of some works in FVMs and CVFEMs. As pointed out by these authors, the formulation of CVFEMs involves five basic steps: (1) discretization of the domain of interest into elements; (2) further discretization of the domain into control volumes that surround the nodes in the finite element mesh, as shown in Figure 1; (3) definition of element-based interpolation functions for variables and physical properties of the fluid; (4) derivation of algebraic equations by using the sub-domain weighted residual method; and (5) choice of a procedure to solve the system of algebraic equations. In this work, these basic steps were applied to an isoparametric quadrilateral nine-noded element for velocity field and four-noded for pressure field (it is known as unequal-order) in structured meshes. The quadrilateral element used can be deformed to fit irregular contours of the domain. Each element of the physical domain is mapped into one element of reference, the master element, defined on a local system of coordinates as can be seen in Figure 2 in order to simplify the integration of the governing equations.

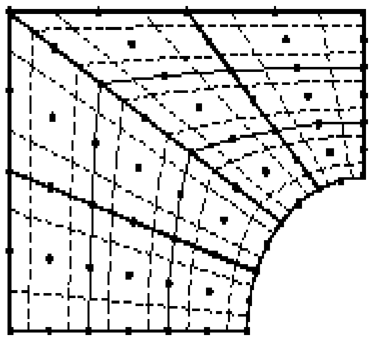

Figure 1 - Meshes of finite elements and control volumes

2. ANALYSIS

2.1 Governing Equations

The unsteady, incompressible viscous flows of Newtonian fluids are governed by the transport of momentum and continuity equations that can be cast in the following general form for the components of velocity u_i and pressure p:

$$\frac{\partial(\rho u_i)}{\partial t} + \frac{\partial(\rho u_j u_i)}{\partial x_j} - \frac{\partial}{\partial x_j}\left[\mu \frac{\partial u_i}{\partial x_j}\right] = S_i - \frac{\partial p}{\partial x_i}; \tag{1}$$

$$\frac{\partial u_i}{\partial x_i} = 0; \tag{2}$$

where ρ and μ are fluid density and dynamic viscosity respectively, S_i is a source term accounting for the other terms not appearing explicitly in equation (1).

The transport of any scalar variable can be written as

$$\frac{\partial(\rho\phi)}{\partial t} + \frac{\partial(\rho u_j \phi)}{\partial x_j} - \frac{\partial}{\partial x_j}\left[\Gamma \frac{\partial \phi}{\partial x_j}\right] = S_\phi; \tag{3}$$

with a proper diffusion coefficient Γ and S_ϕ being a source or sink term.

The above equations are in conservative form used in the FVMs and CVFEMs. These equations must be integrated over each control volume surrounding each node. This is the procedure frequently adopted in the literature. In the present work, the governing equations are integrated over each sub-control volume within elements to form the element matrices. When assembling the global matrix, the principle of mass, momentum and energy conservation is satisfied.

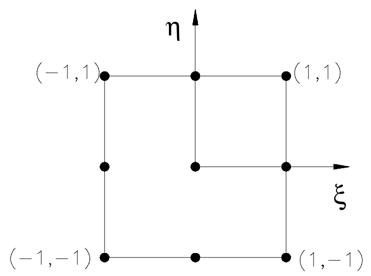

Figure 2(a) - Element in local coordinates

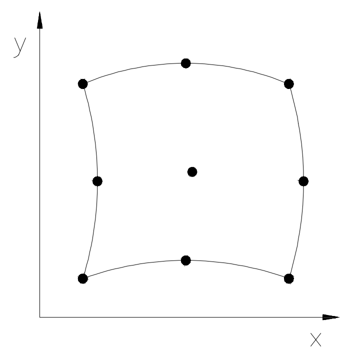

Figure 2(b) - Element in global coordinates

2.2 Finite Element Mesh

In this step, two-dimensional domains were meshed by nine-noded quadrilateral elements. However, the structure of the computational program permits easy use of any other type of element. After discretising the domain, each quadrilateral element is subdivided in nine sub-control-volumes. We have chosen the nine-noded, quadratic, quadrilateral finite element, employed by Raw et al. (1985) for heat conduction; because the desirable attributes of this element for modeling both domains having curved and straight boundaries. Despite the fact that the present element involves more time calculation, one may uses a number of such elements for meshing a domain to obtain the same order of accuracy that could be obtained by using a large number of linear elements. Another advantage of using the nine-noded elements is that domains having curved side may be meshed more accurately.

Integrating equations (1) and (2) over the sub-control volumes of one element gives the following integral form of conservation equations:

$$\int_V \frac{\partial(\rho u_i)}{\partial t} dV + \int_{\delta s} \rho u_j u_i n_j ds - \int_{\delta s} \mu \frac{\partial u_i}{\partial x_j} n_j ds = \int_V \left[S_i - \frac{\partial p}{\partial x_i} \right] dV \tag{4}$$

$$\int_V \frac{\partial u_i}{\partial x_i} dV = 0 \tag{5}$$

where δs is the surface area (contour in 2D) of the control volume, and n_j is the component of a unity outward normal vector to the differential surface area δs in the direction j.

The volume integral of the pressure term in equation (4) and of the continuity, equation (5), were not transformed to surface integrals, because calculation tests shown better results with the volume integrals.

2.3 Interpolation Functions

The integral equations were transformed to a system of algebraic equations, by using interpolating functions for approximation of unknown variables in each element. The interpolating functions employed were defined similarly as in Dhatt & Touzot (1984). The variables and coordinates are approximated in finite element method as

$$u_i = \sum_{\alpha=1}^{nnep} N_\alpha U_{i\alpha} \tag{6}$$

$$p = \sum_{\alpha=1}^{nnel} N_\alpha P_\alpha \tag{7}$$

$$x_i = \sum_{\alpha=1}^{nnep} N_\alpha X_{i\alpha} \tag{8}$$

where N_α are interpolating functions; $U_{i\alpha}$ the velocity components; P_α the pressure and $X_{i\alpha}$ components of the coordinate system at nodes α of a element; nnep and nnel are numbers of nodes of quadratic (parabolic) and linear elements respectively.

The variables defined by equations (6) and (7), and the coordinates obtained by equation (8) were substituted into equations (4) and (5). The following ordinary differential system was obtained:

$$M_{\alpha\beta}\dot{U}_{i\beta} + C_{\alpha\beta}(U_{i\beta})U_{i\beta} - S_{i\alpha\beta}U_{i\beta} + H_{i\alpha\beta}P_\beta = F_{i\alpha} \tag{9}$$

$$D_{i\alpha\beta}U_{i\beta} = 0 \tag{10}$$

where $M_{\alpha\beta}$, $C_{\alpha\beta}$, $S_{i\alpha\beta}$, $H_{i\alpha\beta}$, $D_{i\alpha\beta}$ and $F_{i\beta}$ are coefficients of the mass matrix, the convection matrix, the diffusive matrix, the pressure term matrix, the continuity matrix and the source term vector respectively for a element. More details about such matrices can be found in Campos Silva (1998).

2.4 Modification of the convective term

A technique of upwind developed by Saabas & Baliga (1994) for triangular elements was modified and extended for a nine-noded element by Campos Silva (1998). For implementating the upwind scheme, each finite element method is subdivided by four sub-elements as shown in Figure 3. At each integration point (numbered points ranging from 1 to 16 inside element) the velocity components in the convective term are interpolated taking approximately the direction of flow, in a way that the points upstream have more influence on the integration values.

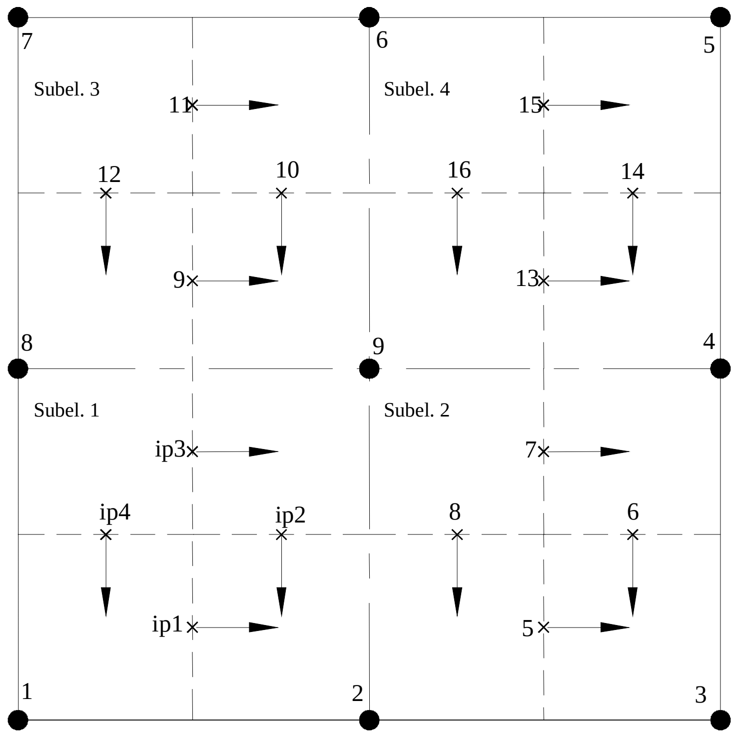

Figure 3 - Element for implementation of upwind

The variables at integration points, taking integration point 1 for example, are interpolated in the form:

$$\text{if } \dot{m}_{ip1} > 0, \qquad \phi_{ip1} = f\phi_{ip4} + (1-f)\Phi_1 \tag{11a}$$

$$\text{where } f = \min\{\max[(\dot{m}_{ip4} / \dot{m}_{ip1}),0],1\}, \tag{11b}$$

$$\text{if } \dot{m}_{ip1} < 0, \qquad \phi_{ip1} = f\phi_{ip2} + (1-f)\Phi_2 \tag{11c}$$

$$\text{where } f = \min\{\max[(-\dot{m}_{ip2} / \dot{m}_{ip1}),0],1\}. \tag{11d}$$

The flux of mass at the integration point i is represented by the symbol $\dot{m}_{ipi}$. Variables at each nodal point from 1 through 9 are represented by capital symbols Φ while variables at each integration point are represented by the symbol ϕ.

In equation (9) the matrix coefficient $C_{\alpha\beta}$ is defined as

$$C_{\alpha\beta} = \oint_{\Gamma_{svc\alpha}} \rho\, N_{\beta} U_j n_j \, d\Gamma \, ; \tag{12}$$

while with use of upwind that coefficient is defined by

$$C_{\alpha\beta} = \sum_{k=1}^{NIP} \dot{m}_k^{\alpha} CC_{k\beta} \tag{13}$$

where

$$\dot{m}_k^{\alpha} = \int_{\Gamma_{k\alpha}} \rho U_j n_j \, d\Gamma \tag{14}$$

and $CC_{k\beta}$ are coefficients of the matrix $[A]^{-1}[B]$, with $[A]$ and $[B]$ being the matrices on the left and right sides respectively of the following equation obtained from equation (11) for all integration points inside a sub-element. In the case of sub-element 1 (subel. 1, Figure 3), it is obtained:

$$\begin{bmatrix} a_{11} & a_{12} & a_{13} & a_{14} \\ a_{21} & a_{22} & a_{23} & a_{24} \\ a_{31} & a_{32} & a_{33} & a_{34} \\ a_{41} & a_{42} & a_{43} & a_{44} \end{bmatrix} \begin{Bmatrix} \phi_{ip1} \\ \phi_{ip2} \\ \phi_{ip3} \\ \phi_{ip4} \end{Bmatrix} = \begin{bmatrix} b_{11} & b_{12} & b_{13} & b_{14} \\ b_{21} & b_{22} & b_{23} & b_{24} \\ b_{31} & b_{32} & b_{33} & b_{34} \\ b_{41} & b_{42} & b_{43} & b_{44} \end{bmatrix} \begin{Bmatrix} \Phi_1 \\ \Phi_2 \\ \Phi_9 \\ \Phi_8 \end{Bmatrix} \tag{15}$$

2.5 Time Discretization

The equations (9) and (10) discretized in time become:

$$\frac{M_{\alpha\beta}}{\Delta t} U_{i\beta}^{n+1} + \lambda (C_{\alpha\beta}^{n+1} - S_{i\alpha\beta}) U_{i\beta}^{n+1} + \lambda H_{i\alpha\beta} P_{\beta}^{n+1} = F_{i\alpha}^{n} \tag{16}$$

$$D_{i\alpha\beta} U_{i\beta}^{n+1} = 0 \tag{17}$$

where

$$F_{i\alpha}^{n} = \frac{M_{\alpha\beta}}{\Delta t} U_{i\beta}^{n} - (1-\lambda)(C_{\alpha\beta}^{n} - S_{i\alpha\beta}) U_{i\beta}^{n} - (1-\lambda) H_{i\alpha\beta} P_{\beta}^{n} \tag{18}$$

and $0 \le \lambda \le 1$. If an implicit scheme is employed, $\lambda = 1$, there is no needing of an initial condition for the pressure field.

We can linearize the inertial terms by computing the matrix $C_{\alpha\beta}$ on the step n instead of updating it on each iteration at the time n+1. The updating of the convection matrix may compute more accurate results; however, it is very time consuming for large problems.

2.6 Procedures of solution

The algebraic system of equations must be assembled element by element to form the global system of equations that can be solved by some method of solution. Depending on the number of degrees of freedom of the problem, the global matrix could become very large and it requires a large storage capacity. The frontal method of solution has been applied. This method solves the global matrix by blocks of specified front size as explained in the book of Taylor & Hughes (1981). Some computational subroutines from Taylor & Hughes (1981) developed for eight-noded elements to Galerkin finite element were modified and used to solve the algebraic systems of equations. Starting from specified velocity and pressure fields, the variables u-v-p may be calculated at any other specified time. The size of the front can be found by trial and error. If the front size is too small, the program sends a message to the user. The smaller the front the faster the calculation of the variables at each time step. However, this method of solution requires a temporary memory space in hard disc to storage data during the calculation. The larger the front size the higher the space on hard disc. The frontal method is appropriate for computation in systems with medium capacity of RAM like personal computers or small workstations, but it's so time consuming because of the temporary storage of data in hard disc and the reading of these data during the solution.

3. APPLICATION OF THE METHOD

In Campos Silva and Moura (1997) some tests of the method for fluid flow simulation were presented without the calculation of heat transfer. In Campos Silva (1998) results for forced and natural convection inside a square cavity were presented. Some of those results for natural convection are also presented in this work. The following system of equations was solved by the method described before:

$$\frac{\partial U}{\partial X}+\frac{\partial V}{\partial Y} \tag{19}$$

$$\frac{\partial U}{\partial t}+\frac{\partial (UU)}{\partial X}+\frac{\partial (VU)}{\partial Y}-\frac{\partial^2 U}{\partial X^2}-\frac{\partial^2 U}{\partial Y^2}+\frac{\partial P}{\partial X}=0 \tag{20}$$

$$\frac{\partial V}{\partial t}+\frac{\partial (UV)}{\partial X}+\frac{\partial (VV)}{\partial Y}-\frac{\partial^2 V}{\partial X^2}-\frac{\partial^2 V}{\partial Y^2}+\frac{\partial P}{\partial Y}=\frac{Ra}{\mathrm{Pr}}\theta \tag{21}$$

$$\frac{\partial \theta}{\partial t}+\frac{\partial (U\theta)}{\partial X}+\frac{\partial (V\theta)}{\partial Y}-\frac{\partial}{\partial X}\left(\frac{1}{\mathrm{Pr}}\frac{\partial \theta}{\partial X}\right)-\frac{\partial}{\partial Y}\left(\frac{1}{\mathrm{Pr}}\frac{\partial \theta}{\partial Y}\right)=0 \tag{22}$$

The boundary conditions for equations above were specified as: $U,V=0$ for all the walls; $\theta=1$ for the wall with $X=0$; $\theta=0$ for the wall with $X=1$. At the top and the bottom walls the heat flux was specified as zero and $P=0$ at center of the cavity. The Prandtl number was set to unity. The dimensionless variables in equations (19) to (22) are defined by

$$X_i = \frac{x_i}{L}, \quad U_i = \frac{u_i L}{\nu}, \quad t = \frac{t^* \nu}{L^2}, \quad P = \frac{(p - p_0)L^2}{\rho_0 \nu^2}, \tag{23a}$$

$$\theta = \frac{T - T_r}{\Delta T}, \; \Pr = \frac{\nu}{\alpha}, \quad Ra = \frac{g \beta \Delta T L^3}{\alpha \nu}. \tag{23b}$$

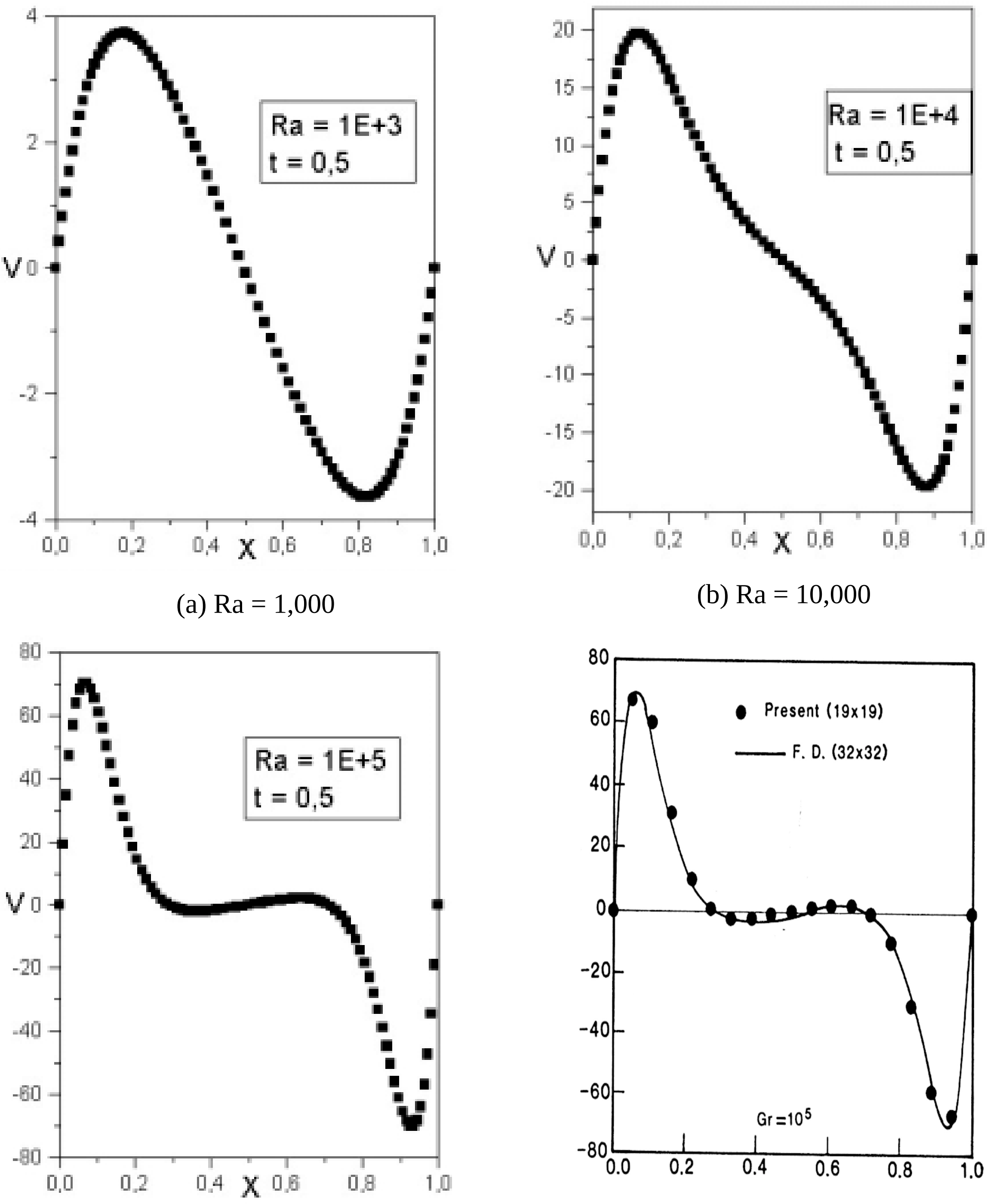

(a) Ra = 1,000 (b) Ra = 10,000

(c) Ra = 100,000 (d) Ra = 100,000, Kettleborough et al. (1989)

Figure 4 - Vertical V velocity along X-axis for Y = 0.5.

Figure 4 shows the results for the V-component of the velocity field at the horizontal centerline of the cavity. The items (c) and (d) compare qualitatively the results of the present work with results from Kettleborough et al. (1989). The Figures 5 and 6 show results for streamlines and isothermal lines respectively compared, qualitatively, with results from Ramaswamy (1988). The streamlines and isothermal lines were obtained by solving the Poisson equation for the stream function and energy equation for the temperature applying the present method. The grid used for the calculation was of 40 by 40 elements along of the axes, which correspond to 81 by 81 points over each axis X or Y.

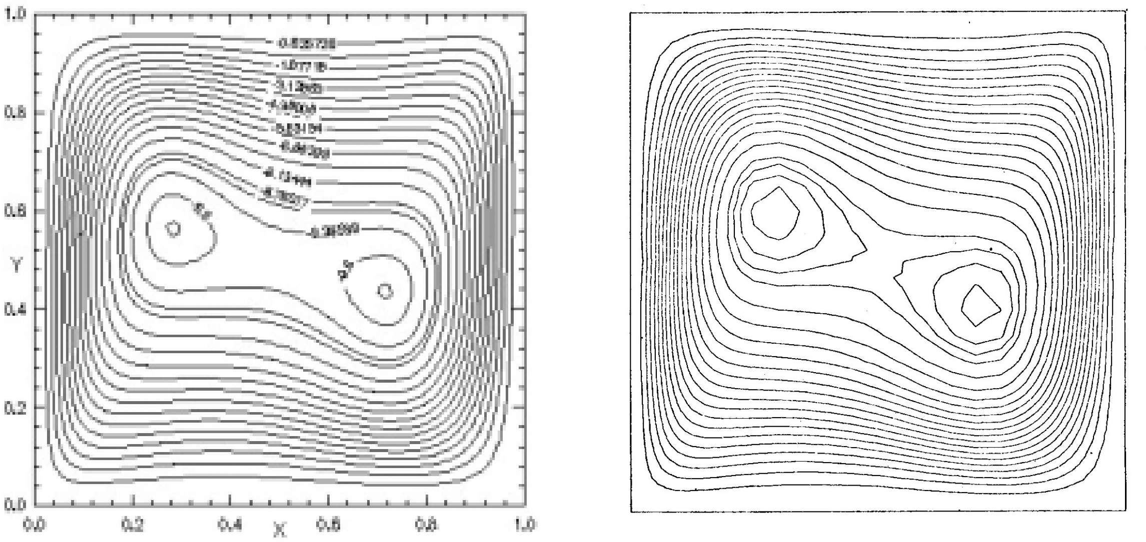

Ra = 100,000 (this work) Ra = 100,000 (Ramaswamy, 1988)

Figure 5 - Streamlines at t = 0.5

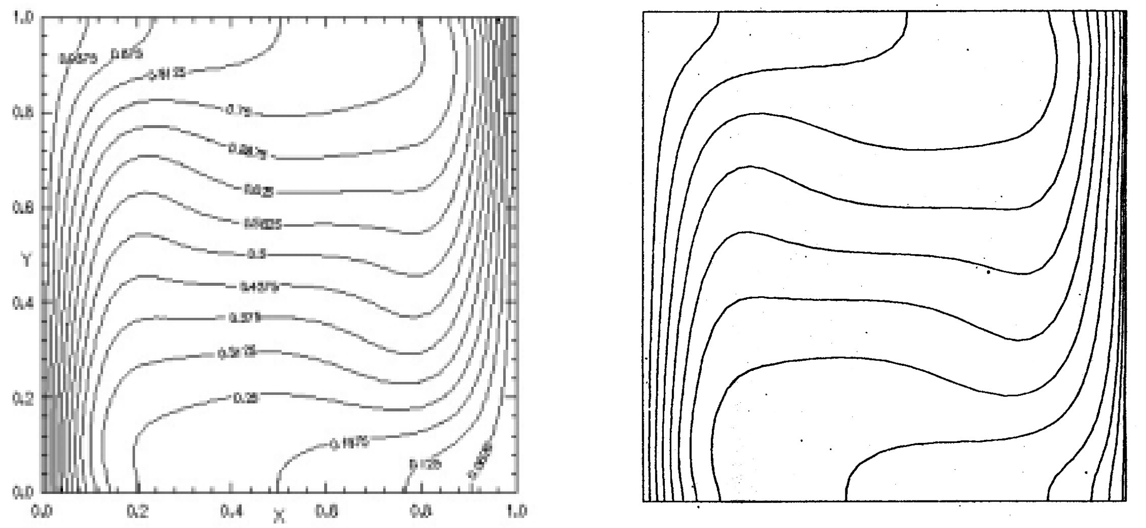

Ra = 100,000 (this work) Ra = 100,000 (Ramaswamy, 1988)

Figure 6 - Isothermal lines at t = 0,5

4. CONCLUSIONS

In the present work, results of a CVFEM implementation for unsteady, incompressible and viscous fluid flow using nine-noded elements were obtained. However, the structure of the numerical code permits the easy extension for other types of elements. The comparisons of the present results and results from the literature, for the Rayleigh numbers specified, show satisfactory agreement. The results from the literature were obtained by other CVFEMs or other numerical methods. Some tests of the upwind technique implemented shown that some refinement of it is still necessary and the solution method for solving the system of algebraic equations needs to be improved to reduce the computation time in more complex problems.

REFERENCES

Baliga, B.R. & Patankar, S.V., 1980, A new finite-element formulation for convection-diffusion problems, Numerical Heat Transfer, vol. 3., pp. 393-409.

Baliga, B.R. & Patankar, S.V., 1983, A control volume finite-element method for two-dimensional fluid flow and heat transfer, Numerical Heat Transfer, vol. 6, pp. 245-261.

Banaszek, J., 1989, Comparison of control volume and Galerkin finite element methods for diffusion-type problems, Numerical Heat Transfer, V. 16, p. 59-78.

Campos Silva, J.B. & Moura, L.F.M., 1997, Numerical simulation of fluid flow by the control volume-finite element method. Proceedings (in CD-ROM) of the XIV Brazilian Congress of Mechanical Engineering - COBEM97, December 8-12, Bauru-SP, Brazil, paper code 041, 8p.

Campos Silva, J.B., Vieira, E.D.R. & Moura, L.F.M., 1998, Control volume-finite element and flow visualization methods applied for unsteady viscous flow past a circular cylinder. Anais do V Congresso de Engenharia Mecânica do Norte-Nordeste, October 27-30, Fortaleza, CE, Brazil, Vol II, pp. 80-87.

Campos Silva, J.B., 1998, Numerical simulation of fluid flow by the finite element method based on control volumes, Doctorate Thesis (in Portuguese), State University of Campinas, Campinas, São Paulo, Brazil.

Dhatt, G. & Touzot, G., 1984, Une Presentation de la Méthode des Éléments Finis, Deuxieme Édition, Maloine S.A. Éditeur, Paris.

Kettleborough, C.F., Husain, S.R. & Prakash, C., 1989, Solution of fluid flow with the vorticity-streamfunction formulation and the control-volume-based finite-element method, Numerical Heat Transfer, Part B, vol. 16, pp.31-58.

Ramaswamy, B., 1988, Finite element solution for advection and natural convection flows. Computer and Fluids, V. 16 No. 4, pp. 349-388.

Raw, M.J & Schneider, G.E., 1986, A skewed, positive influence coefficient up-winding procedure for control-volume-based finite-element convection-diffusion computation. Numerical Heat Transfer, vol. 9, pp. 1-26.

Raw, M.J., Schneider, G.E. & Hassani, V., 1985, A nine-noded quadratic control-volume-based finite element for heat conduction, J. Spacecraft, vol. 22, No. 5, pp.523-529.

Saabas, H.J. & Baliga, B.R., 1994, Co-located equal-order control-volume finite-element method for multidimensional, incompressible, fluid flow - Part I: Formulation, Numerical Heat Transfer, Part B, vol. 26, pp.381-407.

Saabas, H.J. & Baliga, B.R., 1994, Co-located equal-order control-volume finite-element method for multidimensional, incompressible, fluid flow - Part II: Verification, Numerical Heat Transfer, Part B, vol. 26, pp.409-424.

Taylor, C. & Hughes, T.G., 1981, Finite Element Programming of the Navier-Stokes Equations, Pineridge Press Ltd, Swansea, U.K.